

Exactly solvable models and ultracold Fermi gases

M. T. Batchelor^{1,2}, A. Foerster^{3‡}, X.-W. Guan¹ and C. C. N. Kuhn³

¹ Department of Theoretical Physics, Research School of Physics and Engineering, Australian National University, Canberra ACT 0200, Australia

² Mathematical Sciences Institute, Australian National University, Canberra ACT 0200, Australia

³ Instituto de Física da UFRGS, Av. Bento Gonçalves 9500, Porto Alegre, RS, Brazil

Abstract. Exactly solvable models of ultracold Fermi gases are reviewed via their thermodynamic Bethe Ansatz solution. Analytical and numerical results are obtained for the thermodynamics and ground state properties of two- and three-component one-dimensional attractive fermions with population imbalance. New results for the universal finite temperature corrections are given for the two-component model. For the three-component model, numerical solution of the dressed energy equations confirm that the analytical expressions for the critical fields and the resulting phase diagrams at zero temperature are highly accurate in the strong coupling regime. The results provide a precise description of the quantum phases and universal thermodynamics which are applicable to experiments with cold fermionic atoms confined to one-dimensional tubes.

PACS numbers: 02.30.Ik, 03.75.Ss, 03.75.Hh, 64.70.Tg

1. Introduction

The experimental realization of Bose-Einstein condensates in dilute atomic gases [1–3] led to an explosion of ongoing research in ultracold matter physics. A remarkable development was the creation of the first molecular condensate in an ultracold degenerate Fermi gas [4, 5], after which the condensation of fermionic pairs was soon detected and shown to be a superfluid [6]. A relevant question in this fermionic context is if superfluidity can persist in a Fermi gas with imbalanced spin population. In principle, superfluidity may still occur in a mismatched case, and some theories with unusual pairings and exotic phases have been proposed, such as the Fulde-Ferrell-Larkin-Ovchinnikov (FFLO) phase, among others [7, 8]. Subsequently the search for experimental confirmation of these new phases has been conducted by different groups [9, 10]. Until now, however, only paired and polarized phases have been detected in three dimensions.

‡ Corresponding author. Email:angela@if.ufrgs.br

Further remarkable developments have involved the optical confinement of ultracold atoms to one dimension (1D), whereby atoms are trapped and cooled in an array of 1D tubes. These systems include bosonic Rb atoms [11, 12] and fermionic ^{40}K atoms [13]. The most recent experimental breakthroughs involve 1D Rb atoms in the attractive regime [14] and the realization of a 1D spin-imbalanced attractive Fermi gas of ^6Li atoms under the degenerate temperature [15]. This experimental work in 1D has highlighted the fundamental nature of exactly solvable models of quantum many-body systems. In particular, the Bethe Ansatz (BA) integrable models of Lieb and Liniger [16] for spinless bosons and of Yang [17] and Gaudin [18] for two-component fermions. The experimental work has further highlighted the deep and enduring significance of the BA [19]. More general BA integrable multi-component fermions were initially studied by Sutherland [20]. In this paper we examine the BA integrable two- and three-component attractive 1D Fermi gases with population imbalance. We shall see that these ultracold Fermi gases may be used to create nontrivial and exotic phases of matter. They also pave the way for the direct observation and further study of FFLO-like states.

2. Two-component attractive Fermi gas with polarization

2.1. The model

We begin by reviewing the exactly solved two-component model, with Hamiltonian [17, 18]

$$\mathcal{H} = -\frac{\hbar^2}{2m} \sum_{i=1}^N \frac{\partial^2}{\partial x_i^2} + g_{1D} \sum_{1 \leq i < j \leq N} \delta(x_i - x_j) - \frac{1}{2} H (N_{\uparrow} - N_{\downarrow}) \quad (1)$$

which describes N δ -interacting spin- $\frac{1}{2}$ fermions of mass m constrained by periodic boundary conditions to a line of length L and subject to an external magnetic field H . The inter-component interaction g_{1D} can be tuned from strongly attractive to strongly repulsive via Feshbach resonance and optical confinement. The interaction is attractive for $g_{1D} < 0$ and repulsive for $g_{1D} > 0$. Here we will focus on the strongly attractive case, since this regime can be experimentally reached in 1D [15]. For convenience, we define $c = mg_{1D}/\hbar^2$ and a dimensionless interaction strength $\gamma = c/n$ for the physical analysis, with linear density $n = N/L$.

The model (1), which exhibits $SU(2)$ symmetry, was solved independently by Yang [17] and Gaudin [18] using the nested BA. The energy eigenspectrum is given by

$$E = \frac{\hbar^2}{2m} \sum_{j=1}^N k_j^2, \quad (2)$$

where the quasimomenta $\{k_j\}$ of the fermions, satisfy the BA equations [17,18]

$$\begin{aligned} \exp(ik_j L) &= \prod_{\ell=1}^M \frac{k_j - \Lambda_\ell + ic/2}{k_j - \Lambda_\ell - ic/2}, \\ \prod_{\ell=1}^N \frac{\Lambda_\alpha - k_\ell + ic/2}{\Lambda_\alpha - k_\ell - ic/2} &= - \prod_{\beta=1}^M \frac{\Lambda_\alpha - \Lambda_\beta + ic}{\Lambda_\alpha - \Lambda_\beta - ic}, \end{aligned} \quad (3)$$

for $j = 1, \dots, N$ and $\alpha = 1, \dots, M$, with M the number of spin-down fermions. Here $\{\Lambda_\alpha\}$ are the rapidities for the internal spin degrees of freedom.

The solutions to the BA equations (3) provide the ground state properties and the elementary excitations of the model. It was shown [21,22] that the distribution of the quasimomenta in the complex plane for the ground state involves bound states, which can be interpreted as BCS-like pairs, and unpaired (excess) fermions. In the thermodynamic limit, i.e., $N, L \rightarrow \infty$ with N/L finite, and at zero temperature, all quasimomenta k_j of N atoms form two-body bound states, i.e., $k_j = \Lambda_j \pm i\frac{1}{2}c$ for $j = 1, \dots, M$, accompanied by the real spin parameter Λ_j [21]. The BA equations (3) then become

$$\begin{aligned} k_j L &= 2\pi I_j + \sum_{l=1}^M \theta\left(\frac{k_j - \Lambda_l}{c}\right), \quad j = 2M + 1, \dots, N \\ 2\Lambda_j L &= 2\pi J_j + \sum_{l=1}^{N-2M} \theta\left(\frac{\Lambda_j - k_l}{c}\right) + \sum_{l=1}^M \theta\left(\frac{\Lambda_j - \Lambda_l}{2c}\right), \quad j = 1, \dots, M. \end{aligned} \quad (4)$$

where $\theta(x) = 2 \arctan 2x$ with $I_j = -(N - 2M - 1)/2, -(N - 2M - 3)/2, \dots, (N - 2M - 1)/2$ and $J_j = -(M - 1)/2, \dots, (M - 3)/2, (M - 1)/2$.

Introducing the density of unpaired fermions $\rho(k) = dI_j(k)/Ldk$ and the density of pairs $\sigma(\Lambda) = dJ_j(\Lambda)/Ld\Lambda$ it follows that

$$\begin{aligned} \rho(k) &= \frac{1}{2\pi} - \frac{1}{2\pi} \int_{-B}^B \frac{|c|\sigma(\Lambda)d\Lambda}{c^2/4 + (k - \Lambda)^2}, \\ \sigma(\Lambda) &= \frac{1}{\pi} - \frac{1}{2\pi} \int_{-B}^B \frac{2|c|\sigma(\Lambda')d\Lambda'}{c^2 + (\Lambda - \Lambda')^2} - \frac{1}{2\pi} \int_{-Q}^Q \frac{|c|\rho(k)dk}{c^2/4 + (\Lambda - k)^2} \end{aligned} \quad (5)$$

in terms of which the total number of particles, the magnetization and the ground state energy per unit length are given by

$$n = 2 \int_{-B}^B \sigma(\Lambda)d\Lambda + \int_{-Q}^Q \rho(k)dk, \quad (6)$$

$$M^z = \frac{1}{2}(n_\uparrow - n_\downarrow) = \frac{1}{2} \int_{-Q}^Q \rho(k)dk, \quad (7)$$

$$\frac{E}{L} = \int_{-B}^B (2\Lambda^2 - c^2/2) \sigma(\Lambda)d\Lambda + \int_{-Q}^Q k^2 \rho(k)dk. \quad (8)$$

Here the integration boundary Q characterises the Fermi momentum in quasimomentum space and B is the Fermi momentum in spin rapidity space.

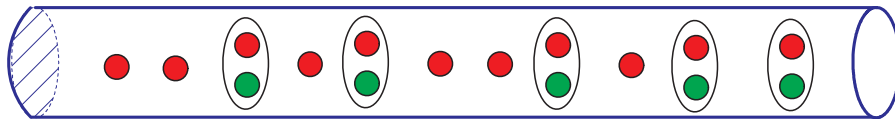


Figure 1. Schematic representation showing the mixture of bound pairs and excess fermions in the strongly attractive regime.

The BA equations (5) are essential to understanding the ground state properties of the model. The integration boundaries implicitly depend on the total number of particles and the magnetization. The strong coupling expansion for the ground state energy per unit length

$$\begin{aligned} \frac{E}{L} \approx & \frac{\hbar^2 n^3}{2m} \left\{ -\frac{(1-P)\gamma^2}{4} + \frac{P^3 \pi^2}{3} \left[1 + \frac{4(1-P)}{|\gamma|} \right] \right. \\ & \left. + \frac{\pi^2 (1-P)^3}{48} \left[1 + \frac{(1-P)}{|\gamma|} + \frac{4P}{|\gamma|} \right] \right\} \end{aligned} \quad (9)$$

has been obtained by using the discrete BA equations (3) [22] or by iteration with the integral equations [23]. Here the polarization P is defined by $P = (N_\uparrow - N_\downarrow)/N$ and the binding energy is $\epsilon_b = \hbar^2 n^2 \gamma^2 / 4m$. The explicit relation between the polarization and the external field H is given further below in equation (16). In this strong coupling region, the system behaves like a mixture of bound pair composites and excess single particles. The form of the ground state energy (9) reveals the nature of weak pair-pair attractive interaction and pair-unpair attractive interaction. A schematic representation of this mixture is depicted in Figure 1.

2.2. Thermodynamic Bethe Ansatz

The thermodynamic properties as well as quantum phase transitions in this model system can be analyzed through the Thermodynamic Bethe Ansatz (TBA). This method was originally proposed by Yang and Yang [24] for spinless bosons and received important contributions for fermions by Takahashi [25], among others [26]. The basic idea of the method is that in the thermodynamic limit we can consider a continuous distribution function for the BA roots. The equilibrium state can be obtained by the condition of minimizing the Gibbs free energy G ,

$$G = E - HM^z - \mu N - TS, \quad (10)$$

where μ is the chemical potential and S the entropy.

This procedure gives rise to a set of coupled nonlinear equations, the TBA equations, for the dressed energies ϵ^b for paired and ϵ^u for unpaired fermions (see [25–27] for details)

$$\epsilon^b(k) = 2(k^2 - \mu - \frac{1}{4}c^2) + Ta_2 * \ln(1 + e^{-\epsilon^b(k)/T}) + Ta_1 * \ln(1 + e^{-\epsilon^u(k)/T}),$$

$$\begin{aligned}\epsilon^u(k) &= k^2 - \mu - \frac{1}{2}H + Ta_1 * \ln(1 + e^{-\epsilon^b(k)/T}) - T \sum_{m=1}^{\infty} a_m * \ln(1 + \eta_m^{-1}(k)), \\ \ln \eta_n(\lambda) &= \frac{nH}{T} + a_n * \ln(1 + e^{-\epsilon^u(\lambda)/T}) + \sum_{m=1}^{\infty} T_{nm} * \ln(1 + \eta_m^{-1}(\lambda))\end{aligned}\quad (11)$$

where $*$ denotes the convolution integral $(f * g)(\lambda) = \int_{-\infty}^{\infty} f(\lambda - \lambda')g(\lambda')d\lambda'$ and the function η_n is the ratio of string densities, coming from Takahashi's hypothesis that complex quasimomenta group together to form strings in the complex plane [26]. The functions

$$a_m(\lambda) = \frac{1}{2\pi} \frac{m|c|}{(m c/2)^2 + \lambda^2}\quad (12)$$

and $T_{mn}(\lambda)$ can also be found in Takahashi's book [26].

In the limit when $T \rightarrow 0$ the TBA equations reduce to the dressed energy equations

$$\begin{aligned}\epsilon^b(\Lambda) &= 2(\Lambda^2 - \mu - \frac{c^2}{4}) - \int_{-B}^B a_2(\Lambda - \Lambda')\epsilon^b(\Lambda')d\Lambda' - \int_{-Q}^Q a_1(\Lambda - k)\epsilon^u(k)dk, \\ \epsilon^u(k) &= (k^2 - \mu - \frac{H}{2}) - \int_{-B}^B a_1(k - \Lambda)\epsilon^b(\Lambda)d\Lambda.\end{aligned}\quad (13)$$

The Gibbs free energy per unit length at zero temperature can be written in terms of the dressed energies as

$$G(\mu, H) = \frac{1}{\pi} \int_{-B}^B \epsilon^b(\Lambda)d\Lambda + \frac{1}{2\pi} \int_{-Q}^Q \epsilon^u(k)dk,\quad (14)$$

from which the density of fermions and the magnetization (or polarization P) follow via the relations

$$-\partial G(\mu, H)/\partial \mu = n, \quad -\partial G(\mu, H)/\partial H = m_z = nP/2.\quad (15)$$

In general, the dressed energy equations provide a clear picture of band fillings with respect to the field H and the chemical potential μ at arbitrary temperatures [28]. These equations can be analytically solved in some special limits, such as in the strongly attractive regime $|\gamma| \gg 1$ [27] discussed below. For comparison, we also present their numerical solution [29].

2.3. Phase diagram at zero temperature

The set of equations (13), (14) and (15) were solved in [27, 29] for strongly attractive interaction using a lengthy iteration method. To leading order, the explicit form for the external field in terms of the density of fermions, the polarization and the interaction strength is given by

$$H = \frac{\hbar^2 n^2}{2m} \left\{ \frac{\gamma^2}{2} + 2P^2 \pi^2 \left[1 + \frac{4(1-P)}{|\gamma|} - \frac{4P}{3|\gamma|} \right] \right\}$$

$$-\frac{\pi^2(1-P)^2}{8} \left[1 + \frac{4P}{|\gamma|} \right] \}. \quad (16)$$

This equation determines the full phase diagram of the model and the critical values of the external field

$$\begin{aligned} H_{c1} &\approx \frac{\hbar^2 n^2}{2m} \left(\frac{\gamma^2}{2} - \frac{\pi^2}{8} \right), \\ H_{c2} &\approx \frac{\hbar^2 n^2}{2m} \left[\frac{\gamma^2}{2} + 2\pi^2 \left(1 - \frac{4}{3|\gamma|} \right) \right]. \end{aligned} \quad (17)$$

These results for H_{c1} and H_{c2} are obtained from equation (16) by setting the polarization to $P = 0$ and $P = 1$, respectively. The critical fields can be physically interpreted as separating three distinct quantum phases: (i) for $H < H_{c1}$ bound pairs populate the ground state, (ii) for $H > H_{c2}$ a completely ferromagnetic phase occurs, and (iii) for the intermediate range $H_{c1} < H < H_{c2}$ paired and unpaired atoms coexist.

Figure 2 illustrates the phase diagram in the $n - H$ plane for the particular value $|c| = 10$. The dashed lines are plotted from equations (17). The coloured phases are obtained by numerically integrating the dressed energy equations (13). The analytical results coincide well with the numerical boundaries. Here it is also clear that subject to the value of the external field, the system exhibits three quantum phases: a BCS-like fully paired phase; an unpaired, fully polarized phase; and a mixed, partially polarized phase, composed of BCS-like pairs and unpaired (excess) fermions. The mixed phase can be considered as a 1D-analogue of the FFLO phase (see, e.g. [30–33]).

Calculations on the BA integrable model thus lead to a two-shell structure composed of the partially polarized FFLO-type phase in the centre of the trap surrounded by – depending on the strength of the external field – either fully paired or fully polarized wings [27, 34, 35]. This prediction was recently verified by the observation by Liao *et al.* [15] of three distinct phases in experimental measurements of ultracold ${}^6\text{Li}$ atoms in an array of 1D tubes. A number of other authors have also investigated the BA integrable model (1) in the context of the Fermi gas (see, e.g., [36–39]).

2.4. TBA for low temperature

In order to handle with the TBA equations (11) at low temperature, we can employ an expansion in terms of the polylogarithm function, which has so far been applied to the 1D attractive Fermi gases of ultracold atoms up to order $1/c^2$ [39–41]. This approach is widely applicable to 1D many-body systems with quadratic or linear bare dispersions in both the attractive and repulsive regimes. It is also expected that the analytical polylogarithmic function approach will play a central role in unifying the properties of attractive Fermi gases of ultracold atoms with higher symmetries. For example, the TBA equations for the 1D Fermi gases with δ -function attractive interactions and internal spin degrees of freedom may be reformulated according to the charge bound states and spin strings characterizing spin fluctuations [40]. Thus for strong attraction, the spin

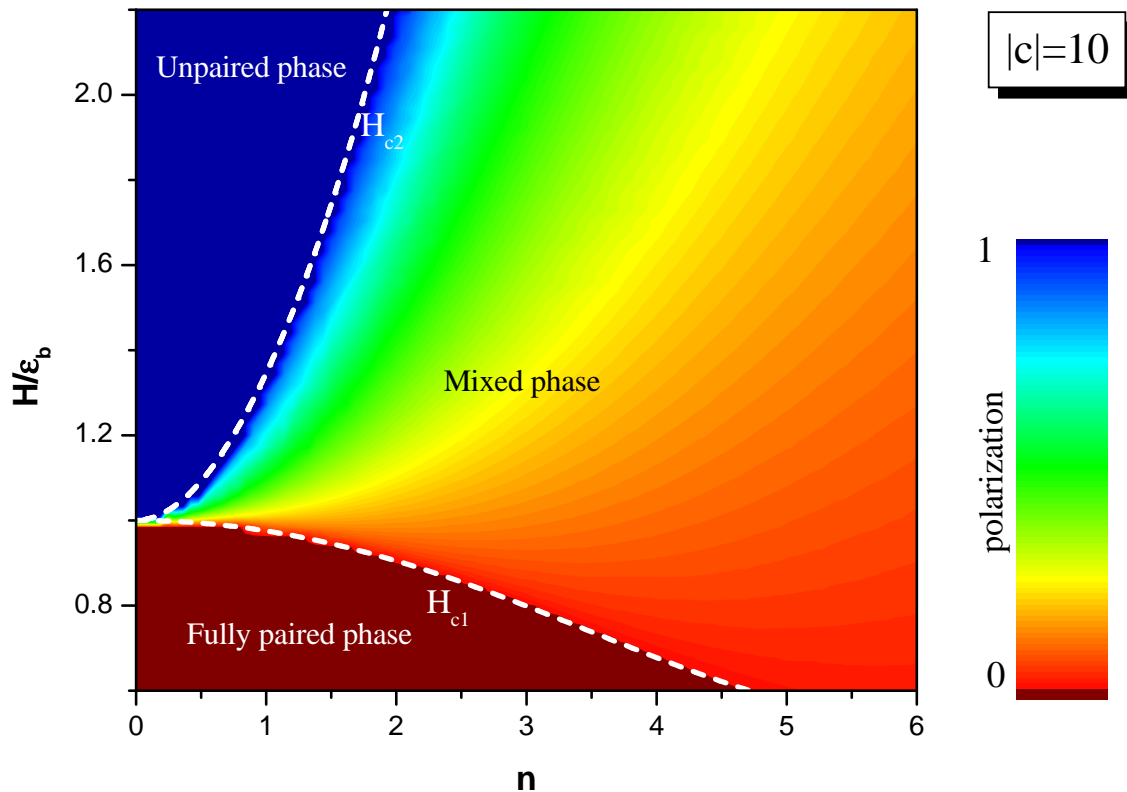


Figure 2. Phase diagram for strong coupling $|c| = 10$ in the $n - H$ plane (from Ref. [29]). Good agreement is found between the analytical results (17) for the critical fields represented by the dashed lines and the numerical solution of the dressed energy equations (13), given by the coloured phases.

fluctuations that couple to non spin-neutral charge bound states are exponentially small and can be asymptotically calculated [40]. Thus the low energy physics is dominated by density fluctuations among the charge bound states. The full phase diagrams and thermodynamics of the 1D attractive Fermi gases can be analytically calculated via this polylogarithm function approach. For spin-1/2 attractive fermions, universal Tomonaga-Luttinger liquid behaviour was identified from the pressure given in terms of polylog functions [39]. Here we discuss some further results, on the universal nature of finite temperature corrections.

For $H \gg k_B T$, where k_B is the Boltzmann constant, we can ignore the exponentially small corrections from the spin bound states and collect the terms up to $1/\gamma^2$ in the TBA equations (11), resulting in the simple form

$$\begin{aligned} \epsilon^b(k) &\approx 2k^2 - A^b(T, H), \\ \epsilon^u(k) &\approx k^2 - A^u(T, H), \end{aligned} \tag{18}$$

where

$$A^b(T, H) = 2 \left[\mu + \frac{1}{4}c^2 - \frac{1}{2|c|} (p^b(T, H) + 4p^u(T, H)) \right] + O\left(\frac{1}{c^3}\right), \quad (19)$$

$$\begin{aligned} A^u(T, H) &= \mu + T \ln(2 \cosh(\frac{H}{2T})) - \frac{2}{|c|} p^b(T, H) \\ &\quad - \frac{J}{4} (1 - B^2) + \frac{3J^2}{32k_B T} (1 - B^4) + O\left(\frac{1}{c^3}\right). \end{aligned} \quad (20)$$

Here we have denoted $B = \tanh \frac{H}{2T}$ and $J = \frac{2}{|c|} p^u(T, H)$. In order to examine the low temperature Luttinger liquid signature, we can safely ignore the exponentially small contribution from the spin wave bound states in the function A^u . Thus integration by parts gives the effective pressures

$$\begin{aligned} p^b(T, H) &= \frac{\sqrt{2}}{\sqrt{\frac{\pi^2 \hbar^2}{2m}}} \int_0^\infty \frac{\sqrt{\epsilon} d\epsilon}{1 + e^{\frac{\epsilon - A^b(T, H)}{k_B T}}}, \\ p^u(T, H) &= \frac{1}{\sqrt{\frac{\pi^2 \hbar^2}{2m}}} \int_0^\infty \frac{\sqrt{\epsilon} d\epsilon}{1 + e^{\frac{\epsilon - A^u(T, H)}{k_B T}}}. \end{aligned} \quad (21)$$

The integrals in (21) can be calculated explicitly using Sommerfeld expansion at low temperatures. We assume that there exist two Fermi seas, i.e., a Fermi sea of bound pairs with a cut-off potential $A^b(T, H)/2$ and a Fermi sea of unpaired fermions with a cut-off potential $A^u(T, H)$. After some lengthy iteration with the relations (15) we obtain the free energy

$$\begin{aligned} F(T, H) &\approx \frac{\hbar^2 \pi^2 n^3 P^3}{6m} \left[1 - \frac{\pi^2}{4} \left(\frac{k_B T}{\mu_0^u} \right)^2 - \frac{\pi^4}{60} \left(\frac{k_B T}{\mu_0^u} \right)^4 \right. \\ &\quad \left. + \frac{4(1-P)}{|\gamma|} \left(1 + \frac{\pi^2}{4} \left(\frac{k_B T}{\mu_0^u} \right)^2 + \frac{2\pi^4}{15} \left(\frac{k_B T}{\mu_0^u} \right)^4 \right) \right] \\ &\quad + \frac{\hbar^2 \pi^2 n^3 (1-P)^3}{2m} \frac{1}{48} \left[1 - \frac{\pi^2}{16} \left(\frac{k_B T}{\mu_0^b} \right)^2 - \frac{\pi^4}{960} \left(\frac{k_B T}{\mu_0^b} \right)^4 \right. \\ &\quad \left. + \left(\frac{(1-P)}{|\gamma|} + \frac{4P}{|\gamma|} \right) \left(1 + \frac{\pi^2}{16} \left(\frac{k_B T}{\mu_0^b} \right)^2 + \frac{\pi^4}{120} \left(\frac{k_B T}{\mu_0^b} \right)^4 \right) \right] \\ &\quad - \frac{1}{2} n P H - \frac{\hbar^2}{2m} n (1-P) \frac{c^2}{4}, \end{aligned} \quad (22)$$

where $\mu_0^u = \frac{\hbar^2 \pi^2 n^2 P^2}{2m}$ and $\mu_0^b = \frac{\hbar^2 \pi^2 n^2 (1-P)^2}{32m}$. We see clearly that the free energy reduces to the ground state energy (9) as $T \rightarrow 0$.

For the temperature $k_B T \ll E_F$, where E_F is the Fermi energy, the spin wave fluctuation is frozen out due to the large magnetic field. The leading low temperature correction to the free energy (22) is

$$F(T, H) = E_0(H) - \frac{\pi C k_B^2 T^2}{6\hbar} \left(\frac{1}{v_b} + \frac{1}{v_u} \right), \quad (23)$$

which belongs to the universality class of the Gaussian model with central charge $C = 1$ [42]. In the above equation, the ground state energy $E_0(H)$ is as given in (9), subject to an additional term $-nPH/2$. The group velocities for bound pairs and unpaired fermions are

$$\begin{aligned} v_b &\approx \frac{v_F(1-P)}{4} \left(1 + \frac{(1-P)}{|\gamma|} + \frac{4P}{|\gamma|} \right), \\ v_u &\approx v_F P \left(1 + \frac{4(1-P)}{|\gamma|} \right), \end{aligned} \quad (24)$$

respectively. Here the Fermi velocity is $v_F = \hbar\pi n/m$. The above result indicates that the low energy physics for 1D strongly attractive fermions in the gapless phase can be described by a two-component Tomonaga-Luttinger liquid model as long as the ferromagnetic spin-spin interaction is frozen out.

In order to recognize a Tomonaga-Luttinger liquid signature in the gapless phase in the low temperature limit, we examine the temperature dependent relations for the magnetization. In general [43], one should expect a magnetization minimum due to a crossover from a Tomonaga-Luttinger liquid with a linear dispersion to a state governed by the nonrelativistic dispersion $\epsilon \propto k^2$. This magnetization minimum does exist in the gapless phase in attractively interacting fermions. We plot the magnetization vs temperature from the free energy (22) in Figure 3, where we observe a clear minimum of the magnetization for different magnetic fields. This comes about due to a crossover from the hardcore bosonic signature of the Tomonaga-Luttinger liquid to polarized free fermions. For further understanding this signature, we derive the magnetization from (23) where we consider the low temperature limit, i.e., $T \rightarrow 0$ (in natural units)

$$m^z = m_0^z - \frac{\pi T^2}{6} \left(\frac{1}{v_b^2} \frac{\partial v_b}{\partial H} + \frac{1}{v_u^2} \frac{\partial v_u}{\partial H} \right), \quad (25)$$

where $m_0^z = \partial E_0(H)/\partial H$. The finite temperature contribution to the magnetization at low temperatures depends on the signs from the term in the brackets of equation (25). This part indicates the existence of a minimum of the magnetization. In the gapless phase two Fermi liquids are coupled through pair-unpaired fermion scattering. The linear field dependent magnetization is a consequence of the fact that the total number of fermions is fixed.

So far we have considered the simplest 1D exactly solvable model in the scenario of ultracold Fermi gases. Generalizations to three and more components can be performed and are discussed in the next sections.

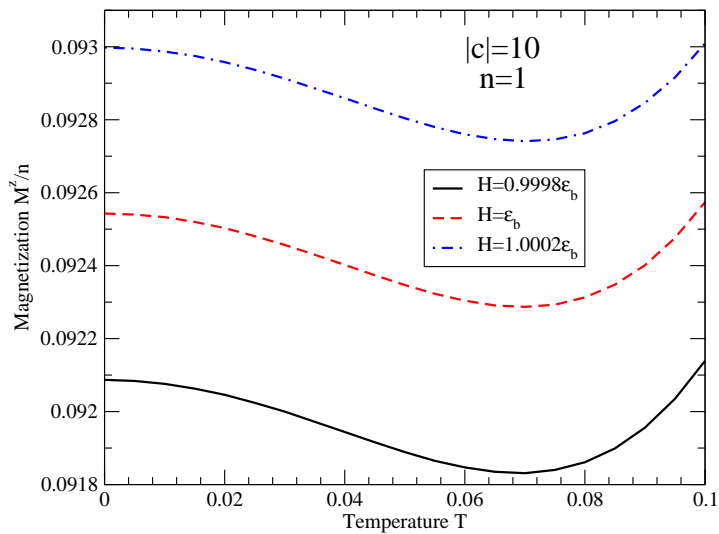


Figure 3. Magnetization m^z vs temperature at different external field values (in the units $2m = \hbar = 1$). The minimum of the magnetization is clearly observed for each field value.

3. Three-component attractive Fermi gas with polarization

3.1. The model

To describe a three-component Fermi gas, the same type of Hamiltonian (1), with a kinetic and a contact potential interacting term, can be considered. However, now the N fermions can occupy three possible hyperfine levels ($|1\rangle$, $|2\rangle$ and $|3\rangle$) and the Zeeman term is expressed in terms of two external fields. The Hamiltonian reads [20]

$$H = -\frac{\hbar^2}{2m} \sum_{i=1}^N \frac{\partial^2}{\partial x_i^2} + g_{1D} \sum_{1 \leq i < j \leq N} \delta(x_i - x_j) + \sum_{i=1}^3 N^i \epsilon_Z^i(\mu_B^i, B). \quad (26)$$

The last term denotes the Zeeman energy, where N^i is the number of fermions in state $|i\rangle$ with Zeeman energy ϵ_Z^i determined by the magnetic moments μ_B^i and the magnetic field B . This term can also be written as $-H_1(N^1 - N^2) - H_2(N^2 - N^3) + N\bar{\epsilon}$, where the unequally spaced Zeeman splitting in three hyperfine levels can be specified by two independent parameters $H_1 = \bar{\epsilon} - \epsilon_Z^1(\mu_B^1, B)$ and $H_2 = \epsilon_Z^3(\mu_B^3, B) - \bar{\epsilon}$, with $\bar{\epsilon}$ the average Zeeman energy. We use the same notation and conventions as in the previous case.

The Hamiltonian (26) exhibits $SU(3)$ symmetry and was solved by Sutherland in the sixties by means of the nested BA [20]. The energy eigenspectrum is again given in terms of the quasimomenta $\{k_i\}$ of the fermions by (2), but now satisfying [20, 21]

$$\exp(ik_j L) = \prod_{\ell=1}^{M_1} \frac{k_j - \Lambda_\ell + ic/2}{k_j - \Lambda_\ell - ic/2},$$

$$\prod_{\ell=1}^N \frac{\Lambda_\alpha - k_\ell + ic/2}{\Lambda_\alpha - k_\ell - ic/2} = - \prod_{\beta=1}^{M_1} \frac{\Lambda_\alpha - \Lambda_\beta + ic}{\Lambda_\alpha - \Lambda_\beta - ic} \prod_{\ell=1}^{M_2} \frac{\Lambda_\alpha - \lambda_\ell - ic/2}{\Lambda_\alpha - \lambda_\ell + ic/2},$$

$$\prod_{\ell=1}^{M_1} \frac{\lambda_\mu - \Lambda_\ell + ic/2}{\lambda_\mu - \Lambda_\ell - ic/2} = - \prod_{\ell=1}^{M_2} \frac{\lambda_\mu - \lambda_\ell + ic}{\lambda_\mu - \lambda_\ell - ic} \quad (27)$$

for $j = 1, \dots, N$, $\alpha = 1, \dots, M_1$, $\mu = 1, \dots, M_2$, with quantum numbers $M_1 = N_2 + 2N_3$ and $M_2 = N_3$. The parameters $\{\Lambda_\alpha, \lambda_m\}$ are the rapidities for the internal hyperfine spin degrees of freedom. For the irreducible representation $[3^{N_3} 2^{N_2} 1^{N_1}]$, a three-column Young tableau encodes the numbers of unpaired fermions ($N_1 = N^1 - N^2$), bound pairs ($N_2 = N^2 - N^3$) and trions ($N_3 = N^3$).

The ground state energy per unit length

$$\begin{aligned} \frac{E}{L} \approx & \frac{\pi^2 n_1^3}{3} \left(1 + \frac{8n_2 + 4n_3}{|c|} \right) - \frac{n_2 c^2}{2} \\ & + \frac{\pi^2 n_2^3}{6} \left(1 + \frac{12n_1 + 6n_2 + 16n_3}{3|c|} \right) - 2n_3 c^2 \\ & + \frac{\pi^2 n_3^3}{9} \left(1 + \frac{12n_1 + 32n_2 + 18n_3}{9|c|} \right) \end{aligned} \quad (28)$$

was obtained in [44] by solving the BA equations (27). Here $n_a = N_a/L$, $a = 1, 2, 3$ are the densities of unpaired fermions, bound pairs and trions, respectively, with the constraint $n = n_1 + 2n_2 + 3n_3$.

The phase diagram of the system for the strongly attractive interaction regime can also be obtained using the dressed energy formalism. For this model, a richer scenario, with more quantum phases, is expected. Indeed, as we shall discuss further below, a trion phase, which consists of three-body bound states, along with a number of mixed phases, are found [44].

3.2. Dressed energy formalism and phase diagrams at zero temperature

In the thermodynamic limit the TBA equations are found by minimizing the Gibbs free energy $G = E + n_1 H_1 + n_2 H_2 - \mu N - TS$. In the limit $T \rightarrow 0$, the dressed energy equations obtained [26, 44, 45] are

$$\begin{aligned} \epsilon^{(3)}(\lambda) &= 3\lambda^2 - 2c^2 - 3\mu - a_2 * \epsilon^{(1)}(\lambda) \\ &\quad - [a_1 + a_3] * \epsilon^{(2)}(\lambda) - [a_2 + a_4] * \epsilon^{(3)}(\lambda) \\ \epsilon^{(2)}(\Lambda) &= 2\Lambda^2 - 2\mu - \frac{c^2}{2} - H_2 - a_1 * \epsilon^{(1)}(\Lambda) \\ &\quad - a_2 * \epsilon^2(\Lambda) - [a_1 + a_3] * \epsilon^{(3)}(\Lambda) \\ \epsilon^{(1)}(k) &= k^2 - \mu - H_1 - a_1 * \epsilon^{(2)}(k) - a_2 * \epsilon^{(3)}(k). \end{aligned} \quad (29)$$

Here $\epsilon^{(a)}$ are the dressed energies and $a_j * \epsilon^{(a)}(x) = \int_{-Q_a}^{+Q_a} a_j(x-y) \epsilon^{(a)}(y) dy$. The negative part of the dressed energies $\epsilon^{(a)}(x)$ for $x \leq |Q_a|$ correspond to the occupied states in the Fermi seas of trions, bound pairs and unpaired fermions, with the positive part of $\epsilon^{(a)}$ corresponding to the unoccupied states. The integration boundaries Q_a characterize the

“Fermi surfaces” at $\epsilon^{(a)}(\pm Q_a) = 0$. The zero-temperature Gibbs free energy per unit length can be written in terms of the dressed energies as

$$G = \sum_{a=1}^3 \frac{a}{2\pi} \int_{-Q_a}^{+Q_a} \epsilon^{(a)}(x) dx, \quad (30)$$

from which physical quantities are obtained through the thermodynamic relations

$$-\frac{\partial G}{\partial \mu} = n, \quad -\frac{\partial G}{\partial H_1} = n_1, \quad -\frac{\partial G}{\partial H_2} = n_2. \quad (31)$$

The dressed energy equations (29) can be analytically solved just in some special limits, such as the strongly attractive coupling regime. This was discussed in [44], where the analytical expressions

$$\begin{aligned} H_1 &= \pi^2 n_1^2 \left(1 - \frac{4n_1}{9|c|} + \frac{8n_2}{|c|} + \frac{4n_3}{|c|} \right) + \frac{10\pi^2 n_2^3}{27|c|} \\ &\quad - \frac{\pi^2 n_3^2}{9} \left(1 + \frac{4n_1}{3|c|} + \frac{32n_2}{9|c|} + \frac{4n_3}{3|c|} \right) + \frac{2c^2}{3}, \\ H_2 &= \frac{\pi^2 n_2^2}{2} \left(1 + \frac{4n_1}{|c|} + \frac{40n_2}{27|c|} + \frac{16n_3}{3|c|} \right) + \frac{16\pi^2 n_1^3}{9|c|} \\ &\quad - \frac{2\pi^2 n_3^2}{9} \left(1 + \frac{4n_1}{3|c|} + \frac{32n_2}{9|c|} + \frac{8n_3}{9|c|} \right) + \frac{5c^2}{6}, \end{aligned} \quad (32)$$

for the energy transfer relations were found (in units of $\hbar^2/2m$). These equations determine the full phase diagram and the critical field values activated by the fields H_1 and H_2 .

Here we numerically solve these equations to confirm the analytical expressions for the physical quantities and the resulting phase diagrams of the model. Basically, for each value of the integration boundaries Q_a , $a = 1, 2, 3$, the equations (29) are converted into a finite size single matrix equation that can be solved using the condition $\epsilon^{(a)}(\pm Q_a) = 0$ to get the dressed energies, the fields and the chemical potential. Then the Gibbs free energy is obtained and from it the polarizations and the linear density are found. Each phase can be identified by properly separating the input in distinct sets containing different combinations of vanishing/non vanishing integration boundaries. For example, in the pure unpaired phase we have $\{Q_2 = Q_3 = 0, Q_1 \neq 0\}$, in the mixed phased composed of unpaired fermions and bound pairs $\{Q_3 = 0, Q_1 \neq 0, Q_2 \neq 0\}$ and so forth. There are seven different combinations and consequently, seven different phases, which are computed and the results collected to generate the complete phase diagrams.

Figures 4 and 5 show the polarizations n_1/n and n_2/n in terms of the fields H_1 and H_2 . There are three pure phases: an unpaired phase A , a pairing phase B and a trion phase C and four different mixtures of these states. A good agreement is observed between the analytical predictions obtained from equations (32) represented by black lines and the numerical solutions obtained by integrating the dressed energy equations (29) represented by white dots.

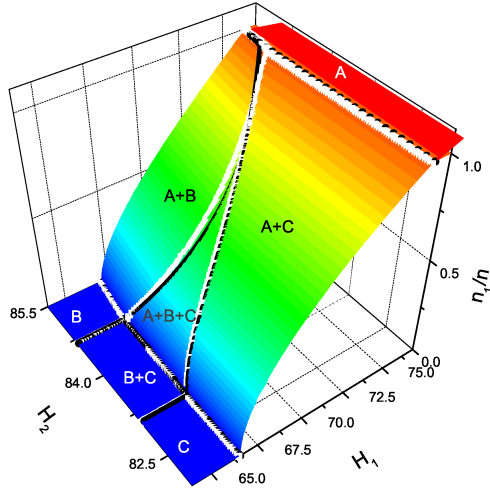


Figure 4. Phase diagram showing the polarization n_1/n versus the fields H_1 and H_2 for strong interaction with $|c| = 10$ and $n = 1$. There are three pure phases: an unpaired phase A, a pairing phase B and a trion phase C and four different mixtures of these states. The black lines are plotted from the analytical results (32) while the white dots correspond to the numerical solutions of the dressed energy equations (29). The numerical phase transition boundaries coincide well with the analytical results.

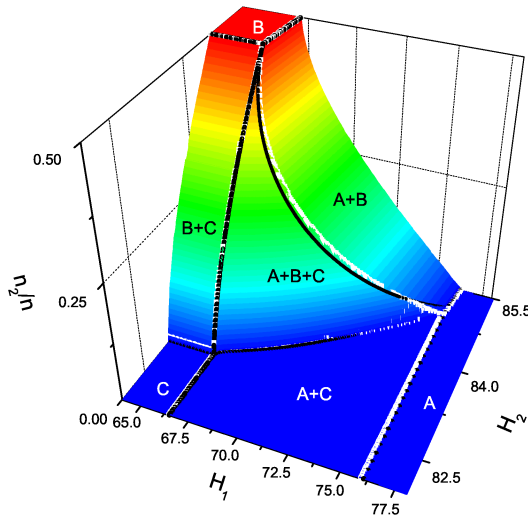


Figure 5. Phase diagram showing the polarization n_2/n versus the fields H_1 and H_2 for strong interaction with $|c| = 10$ and $n = 1$. The black lines plotted from the analytical results (32) are in good agreement with the numerical solutions (white dots) of the dressed energy equations (29).

The ground state energy versus the fields H_1 and H_2 can be determined from the ground state energy (28) with the densities n_1 and n_2 obtained from equation (32).

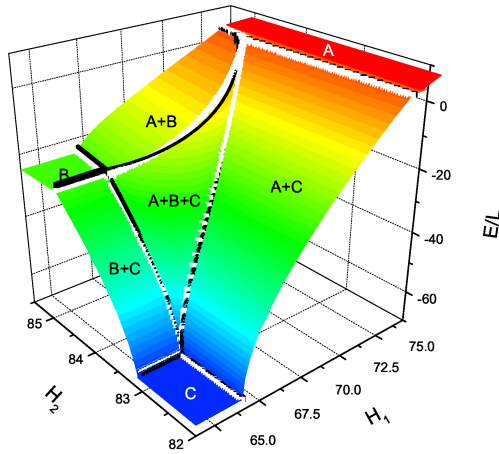


Figure 6. Ground state energy *vs* Zeeman splitting for strong interaction $|c| = 10$ and $n = 1$. Good agreement is found between the analytical results (32) represented by black lines and the numerical solutions obtained by integrating the dressed energy equations (29), represented by white dots.

Figure 6 shows the energy surface for all possible phases shown in Figures 4 and 5. This figure demonstrates the interplay between different physical ground states. For certain values of H_1 and H_2 , a mixture of unpaired fermions, BCS-like pairs and trions ($A + B + C$) populates the ground state.

For low temperature, a similar investigation employing the polylog function can also be performed [41].

4. Conclusion and perspectives

We have examined the two- and three-component attractive 1D Fermi gases with population imbalance via their TBA solution. For the two-component model, we reviewed the strong coupling expansion and the identification of quantum phases. New results for the universal finite temperature corrections were also discussed. For the three-component model, numerical solution of the dressed energy equations confirm that the analytical expressions for the critical fields and the resulting phase diagrams at zero temperature are highly accurate in the strong coupling regime. Both models exhibit rich phase diagrams with a variety of quantum phases. Just as the three distinct phases of the two-component model – the BCS-like paired, fully polarized and partially polarized phases – have been detected by Liao *et al.* [15] in a recent experiment with ultracold ${}^6\text{Li}$ atoms in an array of 1D tubes, it is to be hoped that the more exotic phases of the three-component model – including the trion phase – will be detectable in future experiments.

From the experimental point of view [15], the array of 1D tubes is created within 2D optical lattices. In order to make the lowest transverse mode populated in each tube, the thermal energy $k_B T$ and the Fermi energy are required to be much smaller than the transverse confinement energy. In this sense, the system is well controllable and practicable only for the strongly attractive regime in the quasi-1D trapping. Precisely in this regime, the analytical results may provide direct application to fitting the experimental data, such as the density profiles and phase diagram [46].

Multi-component Fermi gases with more than three species can also be trapped and manipulated. For this type of Fermi gas, bound multi-body clusters are expected to appear above certain critical interaction strengths [47]. The thermodynamic properties and phase diagrams of 1D attractive multicomponent Fermi gases can also be investigated through the solvable models exhibiting $SU(N)$ symmetry [40]. Closed form expressions for the thermodynamics and equation of state of such models will provide further insight towards understanding the nature of many-body effects and different pairing states with higher spin symmetry. The trapping potentials can be accommodated into the equation of state within the local density approximation. It is clear that the Bethe Ansatz will continue to prosper as an essential tool for their description.

Acknowledgments

A. Foerster and C. C. N. Kuhn are supported by CNPq (Conselho Nacional de Desenvolvimento Científico e Tecnológico). The work of M. T. Batchelor and X.-W. Guan is partially supported by the Australian Research Council.

References

- [1] Anderson M H, Ensher J R, Matthews M R, Wieman C E and Cornell E A, 1995 *Science* **269** 198
- [2] Bradley C C, Sackett C A, Tollett J J and Hulet R G, 1995 *Phys. Rev. Lett.* **75** 1687
- [3] Davis K B, Mewes M-O, Andrews M R, van Druten N J, Durfee D S, Kurn D M and Ketterle W, 1995 *Phys. Rev. Lett.* **75** 3969
- [4] Regal C A, Ticknor C, Bohn J L and Jin D S, 2003 *Nature* **424** 47
- [5] Regal C A, Greiner M and Jin D S, 2004 *Phys. Rev. Lett.* **92** 040403
- [6] Zwierlein M W, Abo-Shaeer J R, Schirotzek A, Schunck C H and Ketterle W, 2005 *Nature* **435** 1047
- [7] Fulde P and Ferrell R A, 1964 *Phys. Rev.* **135** A550
Larkin A I and Ovchinnikov Yu N, 1965 *Sov. Phys. JETP* **20** 762
- [8] Liu W V and Wilczek F, 2003 *Phys. Rev. Lett.* **90** 047002
- [9] Zwierlein M W, Schirotzek A, Schunck C H and Ketterle W, 2006 *Science* **311** 492
- [10] Partridge G B, Li W, Liao Y A and Hulet R G, 2006 *Phys. Rev. Lett.* **97** 190407
- [11] Kinoshita T, Wenger T and Weiss D S, 2004 *Science* **305** 1125
- [12] Kinoshita T, Wenger T and Weiss D S, 2005 *Phys. Rev. Lett.* **95** 190406
- [13] Moritz H, Stoferle T, Günter K, Köhl M and Esslinger T, 2005 *Phys. Rev. Lett.* **94** 210401

- [14] Haller E, Gustavsson M, Mark M J, Danzl J G, Hart R, Pupillo G and Nagerl H C, 2009 Science **325** 1224
- [15] Liao Y, Rittner A, Paprotta T, Li W, Patridge G, Hulet R, Baur S and Mueller E, 2010 Nature **467** 567
- [16] Lieb E H and Liniger W, 1963 Phys. Rev. **130** 1605
- [17] Yang C N, 1967 Phys. Rev. Lett. **19** 1312
- [18] Gaudin M, 1967 Phys. Lett. A **24** 55
- [19] Batchelor M T, 2007 Physics Today **60** 36
- [20] Sutherland B, 1968 Phys. Rev. Lett. **20** 98
- [21] Takahashi M, 1970 Prog. Theor. Phys. **44** 899
- [22] Batchelor M T, Bortz M, Guan X -W and Oelkers N, 2006 J. Phys. Conf. Series **42** 5
- [23] Iida T and Wadati M, 2005 J. Phys. Soc. Jpn. **74** 1724
- [24] Yang C N and Yang C P, 1969 J. Math. Phys. **10** 1115
- [25] Takahashi M, 1971 Prog. Theor. Phys. **46** 1388
- [26] Takahashi M, 1999 *Thermodynamics of One-Dimensional Solvable Models* (Cambridge, Cambridge University Press)
- [27] Guan X-W, Batchelor M T, Lee C and Bortz M, 2007 Phys. Rev. B **76** 085120
- [28] Batchelor M T, Guan X-W, Oelkers N and Tsuboi Z, 2007 Adv. Phys. **56** 465
- [29] He J S, Foerster A, Guan X-W and Batchelor M T, 2009 New J. Phys. **11** 073009
- [30] Parish M M, Baur S K, Mueller E J and Huse D A, 2007 Phys. Rev. Lett. **99** 250403
- [31] Zhao E and Liu W V, 2008 Phys. Rev. A. **78** 063605
- [32] Rizzi M, Polini M, Cazalilla M A, Bakhtiari M R, Tosi M P and Fazio R, 2008 Phys. Rev. B. **77** 245105
- [33] Batrouni G G, Huntley M H, Rousseau V G and Scalettar R T, 2008 Phys. Rev. Lett. **100** 116405
- [34] Orso G, 2007 Phys. Rev. Lett. **98** 070402
- [35] Hu H, Liu X J and Drummond P, 2007 Phys. Rev. Lett. **98** 070403
- [36] Iida T and Wadati M, 2007 J. Stat. Mech. P06011
- [37] Iida T and Wadati M, 2008 J. Phys. Soc. Jpn. **77** 024006
- [38] Kakashvili P and Bolech C J, 2009 Phys. Rev. A **79** 041603
- [39] Zhao E, Guan X-W, Liu W V, Batchelor M T and Oshikawa M, 2009 Phys. Rev. Lett. **103** 140404
- [40] Guan X-W, Lee J Y, Batchelor M T, Yin X-G and Chen S, 2010 Phys. Rev. A **82** 021606(R).
- [41] He P, Yin X, Guan X-W, Batchelor M T and Wang Y, arXiv:1009.2283.
- [42] Affleck I, 1986 Phys. Rev. Lett. **56** 746
- [43] Maeda Y, Hotta C and Oshikawa M, 2007 Phys. Rev. Lett. **99** 057205
- [44] Guan X -W, Batchelor M T, Lee C and Zhou H-Q, 2008 Phys. Rev. Lett. **100** 200401
- [45] Schlottmann P, 1997 Int. J. Mod. Phys. **B 11** 355
- [46] Yin X-G, Guan X-W, Chen S and Batchelor M T, in preparation
- [47] Luu T and Schwenk A, 2007 Phys. Rev. Lett. **98** 1973